



Processing bodies and germ granules are distinct RNA granules that interact in *C. elegans* embryos

Christopher M. Gallo^a, Edwin Munro^b, Dominique Rasoloson^a, Christopher Merritt^a, Geraldine Seydoux^{a,*}

^a Department of Molecular Biology and Genetics, Center for Cell Dynamics, Howard Hughes Medical Institute, Johns Hopkins University School of Medicine, 725 N Wolfe Street, 706 PCTB, Baltimore, MD 21205, USA

^b Center for Cell Dynamics, Friday Harbor Laboratories, University of Washington, 620 University Road, Friday Harbor, WA 98250, USA

ARTICLE INFO

Article history:

Received for publication 20 May 2008

Revised 3 July 2008

Accepted 7 July 2008

Available online 16 July 2008

Keywords:

P-bodies
Stress granules
Germ granules
Germ cells
Caenorhabditis elegans

ABSTRACT

In somatic cells, untranslated mRNAs accumulate in cytoplasmic foci called processing bodies or P-bodies. P-bodies contain complexes that inhibit translation and stimulate mRNA deadenylation, decapping, and decay. Recently, certain P-body proteins have been found in germ granules, RNA granules specific to germ cells. We have investigated a possible connection between P-bodies and germ granules in *Caenorhabditis elegans*. We identify PATR-1, the *C. elegans* homolog of the yeast decapping activator Pat1p, as a unique marker for P-bodies in *C. elegans* embryos. We find that P-bodies are inherited maternally as core granules that mature differently in somatic and germline blastomeres. In somatic blastomeres, P-bodies recruit the decapping activators LSM-1 and LSM-3. This recruitment requires the LET-711/Not1 subunit of the CCR4-NOT deadenylase and correlates spatially and temporally with the onset of maternal mRNA degradation. In germline blastomeres, P-bodies are maintained as core granules lacking LSM-1 and LSM-3. P-bodies interact with germ granules, but maintain distinct dynamics and components. The maternal mRNA *nos-2* is maintained in germ granules, but not in P-bodies. We conclude that P-bodies are distinct from germ granules, and represent a second class of RNA granules that behaves differently in somatic and germline cells.

© 2008 Elsevier Inc. All rights reserved.

Introduction

Germ granules are cytoplasmic, RNA-rich organelles specific to germ cells. Although germ granules have been observed in over 80 animal species from rotifers to mammals (Eddy, 1975), their molecular function remains mysterious. Germ granules contain mRNAs and mRNA-binding proteins, suggesting a function in post-transcriptional gene regulation (Seydoux and Braun, 2006). Recently, germ granules have been shown to contain proteins also found in the processing bodies (P-bodies) and stress granules of somatic cells (reviewed in Anderson and Kedersha, 2006). P-bodies were first described as sites of mRNA degradation, and have also been implicated in the inhibition of mRNA translation. The current view is that P-bodies function as temporary holding or triage sites for non-translated mRNAs destined for degradation or translational reactivation (reviewed in Parker and Sheth, 2007). P-bodies contain several proteins implicated in translational repression and activation of mRNA decapping (Dhh1/RCK/p54, Scd6/RAP55, Pat1p, Lsm1-7 and Edc3). P-bodies also contain enzymatic complexes, including the decapping enzyme Dcp2 and its co-subunit Dcp1, the CCR4-NOT deadenylase complex, and Xrn1, a 5' to 3' RNA exonuclease (reviewed in Parker and Sheth, 2007).

Certain P-body components (e.g. Dhh1/RCK/p54, Scd6/RAP55 and XRN1) also localize to stress granules (Anderson and Kedersha, 2006). Stress granules form when somatic cells are exposed to environmental stresses such as heat, UV irradiation and oxidative conditions. Under these stresses, translation of mRNAs encoding housekeeping proteins is halted, and mRNAs move from polysomes to stress granules. Stress granule formation depends on TIA-1, an mRNA-binding protein that promotes the aggregation of modified translation pre-initiation complexes that form the core of stress granules (Kedersha et al., 1999). Stress granules interact with P-bodies in mammalian cells (Kedersha et al., 2005) and TIA-1 can promote the degradation of certain mRNAs (Yamasaki et al., 2007), suggesting that stress granules and P-bodies may function together to regulate the balance of translated, repressed and degraded mRNAs in somatic cells.

P-bodies and stress granules have been characterized best in yeast cells (P-bodies) and/or in mammalian tissue culture cells (P-bodies and stress granules). Whether these structures also exist in germ cells and what their relationships are to germ granules remains unclear. Analyses in *Drosophila*, *Caenorhabditis elegans*, and mice have shown that certain P-body components co-localize with germ granules but also localize to other foci. For example, the *Drosophila* homologues of Dcp1 (dDcp1) and Dhh1/RCK/p54 (Me31B) localize to an area of the oocyte where germ granules are formed (polar plasm), but also localizes with Dcp2 to other granules in nurse cells, which share cytoplasm with the oocyte (Lin et al., 2006; Nakamura et al.,

* Corresponding author. Fax: +1 410 955 9124.

E-mail address: gseydoux@jhmi.edu (G. Seydoux).

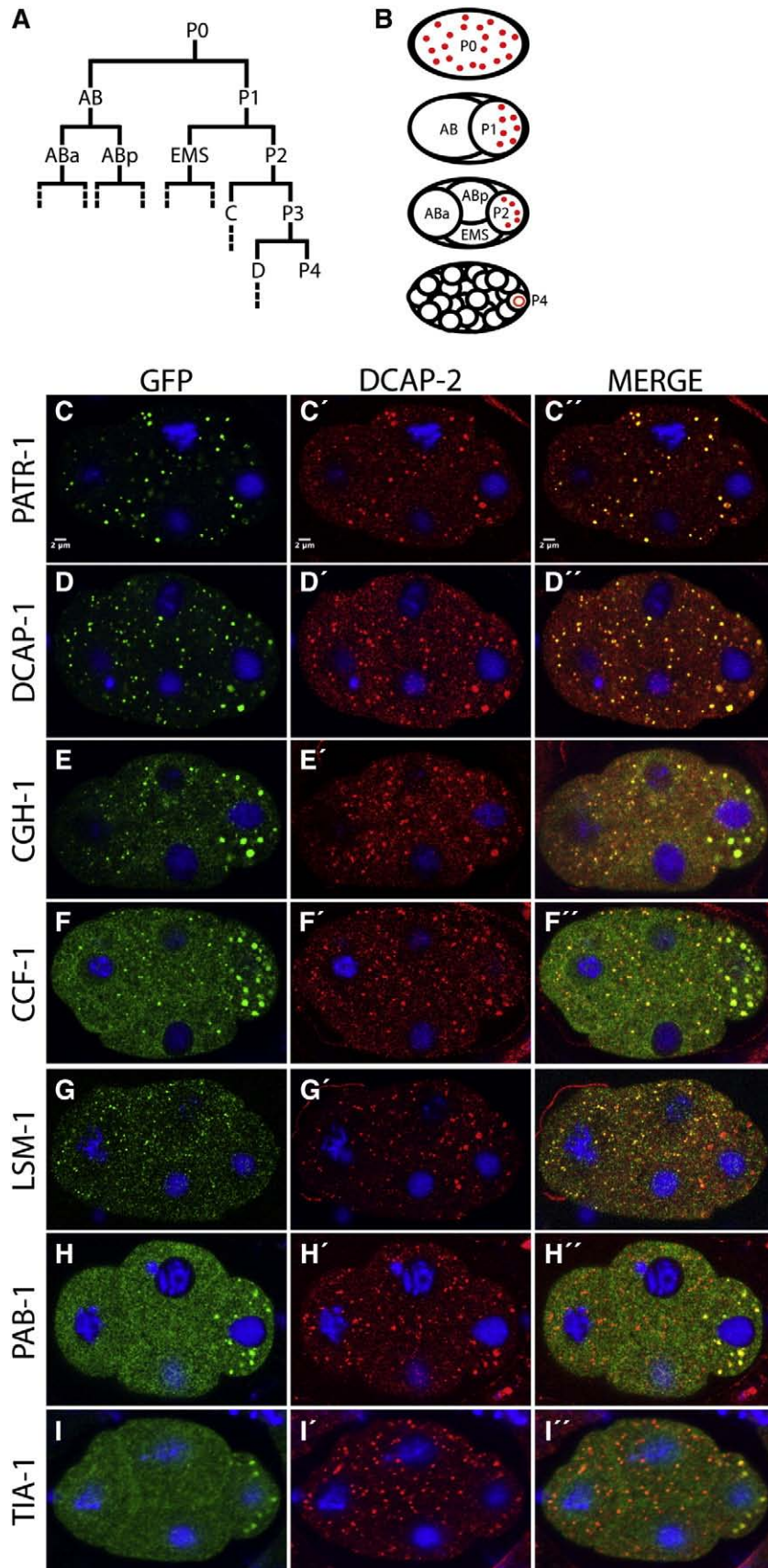


Fig. 1. P-body and stress granule components localize to discrete foci in early embryos. (A) Early embryonic lineage. AB, EMS, C and D are somatic blastomeres, P₀–P₄ are germline blastomeres. P₀–P₃ divide asymmetrically. (B) Schematics of 1, 2, 4 and 28-cell stage embryos. Germ granules are in red. Embryos are oriented with the anterior to the left and posterior to the right in this and all other figures. (C–I''). Confocal images (single focal slices) of fixed 4-cell stage embryos expressing the indicated GFP fusions and double-stained with anti-GFP (green) and anti-DCAP-2 (red) antibodies. All fusions concentrate into foci, and most can also be detected diffusely throughout the cytoplasm (with the possible exception of PATR-1 and DCAP-1, which appear most concentrated in foci).

2001). Similarly, in *C. elegans*, DCAP-1 (Dcp1), DCAP-2 (Dcp2), CGH-1 (Dhh1/RCK/p54) and CAR-1 (Scd6/RAP55) co-localize with the germ granule marker PGL-1 on large granules in germline blastomeres, but also localize to many other smaller granules, most numerous in somatic blastomeres (Audhya et al., 2005; Boag et al., 2005; Lall et al., 2005; Navarro et al., 2001; Squirrell et al., 2006). During mouse spermatogenesis, Dcp1a localizes to many cytoplasmic granules during meiosis, and eventually concentrates in the chromatoid body, the germ granule equivalent of post-meiotic spermatocytes (Kotaja et al., 2006).

We have investigated the relationship between germ granules, P-bodies and stress granules in *C. elegans* embryos. In *C. elegans*, germ granules are called P granules (Strome, 2005), but to avoid confusion with P-bodies we use the term germ granules in this study. Germ granules are present throughout life in the germline of *C. elegans* (with the exception of mature sperm) and are uniquely recognized by the monoclonal antibody K76 (Strome and Wood, 1983). Germ granules contain several constitutive components including the K76 antigen PGL-1, an RGG box protein, and GLH-1 through 4, predicted RNA helicases related to *Drosophila* VASA (Strome, 2005). Several mRNAs have been localized to germ granules in the adult gonad (Schisa et al., 2001), and one maternal mRNA (*nos-2*) is enriched in germ granules in embryos (Subramaniam and Seydoux, 1999). Germ granules in embryos also recruit several RNA binding proteins, including a group of CCCH finger proteins (MEX-5, MEX-6, PIE-1 and POS-1) with complex roles in embryonic polarity and/or germ cell fate (Mello et al., 1996; Schubert et al., 2000; Tabara et al., 1999).

Germ granules segregate asymmetrically during the first embryonic cleavages (Strome, 2005). The zygote (P_0) divides into a larger anterior somatic blastomere AB and a smaller posterior germline blastomere P_1 . P_1 , and its descendents P_2 and P_3 , continue to divide asymmetrically until the birth of P_4 , the germline founder in the 16/24-cell stage (Figs. 1A, B). At each asymmetric division, germ granules are preferentially segregated to the next germline blastomere, so that at each stage the majority of germ granules are present in only one cell. Maternal mRNAs are also preferentially maintained in germline blastomeres, with maternal mRNA degradation starting around the 4-cell stage specifically in somatic blastomeres (Seydoux and Fire, 1994). The simple and reproducible lineage of *C. elegans* makes it possible to follow the segregation of GFP-tagged proteins in live embryos. Here we use a combination of live imaging and confocal microscopy to track P-bodies and germ granules during early cleavages. Our data indicate that P-bodies and germ granules are distinct RNA granules, and suggest parallels between germ granules and the stress granules of somatic cells.

Materials and methods

Nematode strains

C. elegans strains (Table S1) were derived from wild-type Bristol N2 and reared with standard procedures (Brenner, 1974).

Cloning and transgene construction

All transgenes used in this study were driven by the *pie-1* promoter (maternal expression) unless otherwise indicated. Gateway cloning (Invitrogen) was used to generate all constructs (Landy, 1989). Coding sequences were PCR amplified from mixed stage N2 cDNA (*cgh-1*, *lsm-1*, *lsm-3*, *Y46G5A.13* [*tia-1*], *ccf-1*, *pos-1*, *exos-1*, *exos-2*, and *exos-3*) or N2 genomic DNA (*dcap-1*, *pab-1*, *pgl-1*, and *patr-1*) and cloned into pDONR201. *exos-1*, *ccf-1*, and *pgl-1* were cloned with their own 3' UTR. pDONR constructs were recombined into pKC1.01 [to generate N-terminal LAP-tagged (Cheeseman et al., 2004) fusion proteins] or pCM2.03 (to generate N-terminal GFP fusion proteins under the control of their own 3' UTR). mCherry:PATR-1 was

generated by PCR fusion of the mCherry coding sequence to the *patr-1* ORF, and recombining the PCR product into pDONR201. The resulting pDONR vector was recombined into pID2.02.

Transgenes were introduced into worms by microparticle bombardment (Praitis et al., 2001). The mCherry:PATR-1; PGL-1:GFP double-marked line was made by crossing JH2329 (Table S1) to worms expressing PGL-1:GFP driven by the *nmy-2* promoter (Wolke et al., 2007).

RNAi-mediated knockdown

The entire *cgh-1* coding sequence was cloned into pDONR201. Bases 105–1180 of the *mex-5* ORF, bases 795–901 of the *mex-6* ORF, and bases 1384–2209 of the *patr-1* ORF were cloned into pDONR201. All resulting pDONR vectors were recombined into the RNAi feeding vector pCD1.01 and transformed into HT115 bacterial cells. Feeding strains of *ama-1* and *let-711* were obtained from the Ahringer feeding library (Kamath and Ahringer, 2003). Strains were grown at 37 °C in LB + ampicillin (100 µg/mL) then spread on NNGM (nematode nutritional growth media) + ampicillin (100 µg/mL) + IPTG (1 mM) and incubated overnight at room temperature. L4 worms were then placed onto RNAi feeding lawns and incubated at 25 °C for 22–27 h, except for *cgh-1* and *let-711*, which were incubated for 16–19 h. RNAi feeding in *rrf-3* (*pk1426*) worms was performed at 22 °C.

PATR-1 antibody and Western blotting

Affinity purified polyclonal anti-PATR-1 antibodies were generated against the peptide KVSNLHPDQFKYLVLGALNLDLTKR in rabbit (Covance). For western blotting ~75 worms were placed into M9 buffer plus NuPage LDS Sample Buffer (Invitrogen), freeze thawed for 3 cycles, then boiled at 100 °C for 10 min. The samples were then loaded onto 4%–12% SDS-PAGE gel (Invitrogen) and transferred to Immobilon-P membranes (Millipore). Antibody dilutions were as follows: rabbit anti-PATR-1 (1:10,000), mouse anti-alpha-tubulin (1:2,000; Sigma), HRP-conjugated goat anti-rabbit and anti-mouse (1:5,000; Jackson ImmunoResearch). Rabbit anti-PATR-1 was incubated overnight at 4 °C.

Immunostaining, live imaging, and microscopy

Adult hermaphrodites were placed onto polylysine-coated slides and squashed under a coverslip to extrude embryos. Slides were then frozen on dry ice, and the coverslip was removed. Samples were fixed by incubation in –20 °C methanol for 15 min, followed by incubation in –20 °C acetone for 10 min. The samples were blocked for 30 min in PBS+0.1% BSA+0.1% Triton X-100 (PBT). Primary antibody were diluted as follows in PBT: rabbit anti-GFP (1:500; Molecular Probes), mouse anti-GFP (1:250; Molecular Probes), rat anti-DCAP-2 (1:200), rabbit anti-PATR-1 (1:1500), K76 (1:10; DSHB-University of Iowa), and rabbit anti-DsRed (1:250; Clontech). Secondary antibodies were the following: FITC-conjugated goat anti-rabbit and goat anti-mouse (1:25; Jackson ImmunoResearch), Cy3-conjugated goat anti-rabbit (1:50; Jackson ImmunoResearch), Cy3-conjugated goat anti-mouse IgM (1:50; Jackson ImmunoResearch), Alexa 568-conjugated goat anti-rat (1:100; Molecular Probes). All primary antibody incubations were done at room temperature for 1–2 h, except for anti-PATR-1, which was performed at 4 °C overnight. All secondary antibody incubations were performed at room temperature for 0.5–1 h. Wide-field fluorescence images were acquired with a Photometrics Cool Snap HQ digital camera attached to a Zeiss Axio Imager and processed with IPLab software (Scanalytics, Inc.) or Slidebook software (Intelligent Imaging Innovations) and Photoshop CS2. Confocal microscopy images were acquired by a Zeiss LSM 510 confocal laser-scanning microscope and software and processed in ImageJ (NIH) and Photoshop CS2.

Time-lapse movies were acquired using a Biorad Radiance confocal scanhead mounted on a Nikon eclipse 800 upright microscope (60×1.4NA plan apochromat lens, and a zoom factor of 2.0) (Movie 6) or a DeltaVision wide-field epifluorescence microscope (Applied Precision, Issaquah, Wa), using an Olympus 100x, 1.35 NA oil immersion lens (Movie 1–5).

In situ hybridization and FISH

In situ hybridization of *nos-2* mRNA was performed as described previously (Seydoux and Fire, 1994) except that probe hybridization was performed at 46 °C. For FISH experiments, pre-hybridization, hybridization, and post-hybridization wash steps were the same as above. Probe detection was carried using the Fluorescent Antibody Enhancer Set for DIG Detection per the manufacturer's instructions (Roche). Germ granules and mCherry:PATR-1 were detected by incubating samples with K76 (1:100 in PBT) and anti-DsRed (1:250) overnight at 4 °C followed by Cy3-conjugated goat anti-mouse IgM (1:100) or Alexa 647-conjugated goat anti-mouse IgM (1:100) and Cy3-conjugated goat anti-rabbit (1:50) for 30 min at room temperature. Images were acquired with a Photometrics Cool Snap HQ digital camera attached to a Zeiss Axio Imager and processed with Slidebook software and Photoshop CS2.

Quantification

Values in Fig. 7 were obtained by measuring total fluorescence intensity (background subtracted) for each nucleus of the three most proximal oocytes. A minimum of 5 gonad arms per condition were analyzed. Values were averaged and normalized such that wild-type was equal to 1.

Results

Distribution of P-body, stress granule and exosome components in fixed embryos

To examine the localization of P-bodies in *C. elegans* embryos, we cloned the *C. elegans* homologs of six evolutionarily conserved P-body components, DCAP-1 (Dcp1), CGH-1 (Dhh1/RCK/p54), PATR-1 (Pat1p), CCF-1 (CAF1/Pop2 subunit of the CCR4-NOT deadenylase), LSM-1 and LSM-3 (Lsm proteins) and expressed them as GFP fusions in embryos (Materials and Methods). For comparison, we also included in our analysis two proteins typically found in stress granules [TIA-1 and PAB-1 (poly(A) binding protein)] and three exosome subunits (EXOS-1/Csl4, EXOS-2/Rrp4, and EXOS-3/Rrp40). The exosome is a multi-subunit complex that degrades RNAs in the 3'–5' direction. Exosome components do not localize to P-bodies, which instead contain the 5' to 3' exonuclease Xrn1 (Bashkirov et al., 1997; Sheth and Parker, 2003). The localization of each fusion was examined by confocal microscopy in 4-cell stage embryos fixed and double-stained with antibodies against GFP and DCAP-2 (P-body marker, Lall et al., 2005) (Fig. 1). The localizations of DCAP-1, DCAP-2 and CGH-1 have been described previously (Lall et al., 2005; Navarro et al., 2001; Squirrell et al., 2006).

All P-body and stress granule GFP fusions localized to cytoplasmic foci (Fig. 1). Some fusions appeared almost exclusively in foci (DCAP-1 and PATR-1), whereas others were also detected diffusely in the cytoplasm (CGH-1, LSM-1/-3, CCF-1, PAB-1, and TIA-1). DCAP-1, CGH-1, PATR-1, and CCF-1 fusions formed foci in both somatic and germline blastomeres. In contrast, LSM-1 and LSM-3 fusions only localized to foci in somatic blastomeres (Fig. 1 and Fig. S1A), and PAB-1 and TIA-1 fusions only localized to foci in germline blastomeres (Figs. 1H, I). In contrast, exosome GFP fusions were diffusely distributed in the cytoplasm and nuclei in all blastomeres and did not form distinct foci (Fig. S1B and data not shown).

One concern when using transgenics to report on the localization of RNP complexes is that overexpression of the tagged fusions could lead to artifacts in RNP composition. Several lines of evidence, however, suggest that this is not the case here. First, our transgenes were introduced in the genome by bombardment, a technique that most often results in single or low-copy insertion events (Praitis et al., 2001) and is therefore unlikely to cause gross overexpression. Second, not all GFP fusions localized to all granules, demonstrating specificity. Third, GFP fusions to P-body components localized to foci positive for endogenous DCAP-2 (Figs. 1C'–G"), suggesting that the fusions associate with endogenous P-bodies. Finally, in the case of DCAP-1, CGH-1 and PATR-1, the GFP patterns matched those obtained by immunostaining against the corresponding endogenous proteins (Lall et al., 2005; Navarro et al., 2001; Squirrell et al., 2006; this study, see below).

Most foci were ~1 μm or smaller, except for a subset in germline blastomeres that appeared larger (~1–2 μm). To determine whether these larger foci correspond to germ granules, we repeated the double-staining experiments with K76, a monoclonal antibody that recognizes the germ granule component PGL-1 (Kawasaki et al., 1998). With the exception of GFP:TIA-1 (and GFP:PGL-1) foci which were all K76-positive, all P-body component GFP fusions localized to both K76-positive and K76-negative (arrow heads) foci in germline blastomeres (Fig. 2). This was also true for POS-1, a CCCH finger protein known to associate with germ granules in embryos (Tabara et al., 1999). For those fusions that gave the strongest foci-to-cytoplasm ratio (GFP: PATR-1, GFP:DCAP-1, GFP:CGH-1), close inspection of K76 foci revealed that co-incidence with K76 was often imperfect (Table 1). In many cases, the GFP and K76 signals overlapped only partially, in complex patterns suggesting a heterogeneous granule or granules. Similar results were obtained for endogenous DCAP-2 (Table 1). In the case of GFP:PATR-1, we observed very few examples of perfect overlap, and instead observed several clear examples of GFP:PATR-1 foci docked around a single larger K76 granule (Table 1 and Fig. 2). These results suggest that PATR-1 is not a germ granule component, but is a component of a second granule type present in both somatic and germline blastomeres.

To verify this pattern, we generated an antibody to PATR-1 and examined the distribution of endogenous PATR-1 in wild-type embryos containing no GFP transgene. The specificity of the PATR-1 antibody was confirmed in western and immunostaining experiments comparing embryos depleted for PATR-1 by RNAi to untreated embryos (Fig. S2). As observed with the GFP:PATR-1 fusion, we found that PATR-1 localizes to numerous foci in both somatic blastomeres and germline blastomeres. Double-staining experiments with K76 confirmed that PATR-1 granules in germline blastomeres rarely overlap with germ granules (Fig. 3D and Table 1). Most were found far from germ granules and the remainder overlapped partially or were "docked" around a single germ granule. The only difference that we noticed between endogenous PATR-1 and GFP:PATR-1 was that GFP:PATR-1 granules were larger and were docked around germ granules less frequently (Table 1 and data not shown).

We conclude that germline blastomeres contain at least two types of granules, germ granules, which contain PGL-1 (the K76 antigen) and TIA-1 but no PATR-1, and a second granule containing PATR-1 but no PGL-1 or TIA-1. We provisionally call the latter PATR-1 granules, for the only component that most uniquely localizes to these PGL-1-negative structures. In addition to their unique components, germ granules and PATR-1 granules share some components, in particular CGH-1, and to a lesser extent DCAP-1 and DCAP-2, which appear less frequently in germ granules (Table 1).

Dynamics in germline blastomeres

To investigate further the relationship between PATR-1 granules and germ granules, we examined the dynamics of mCherry:PATR-1

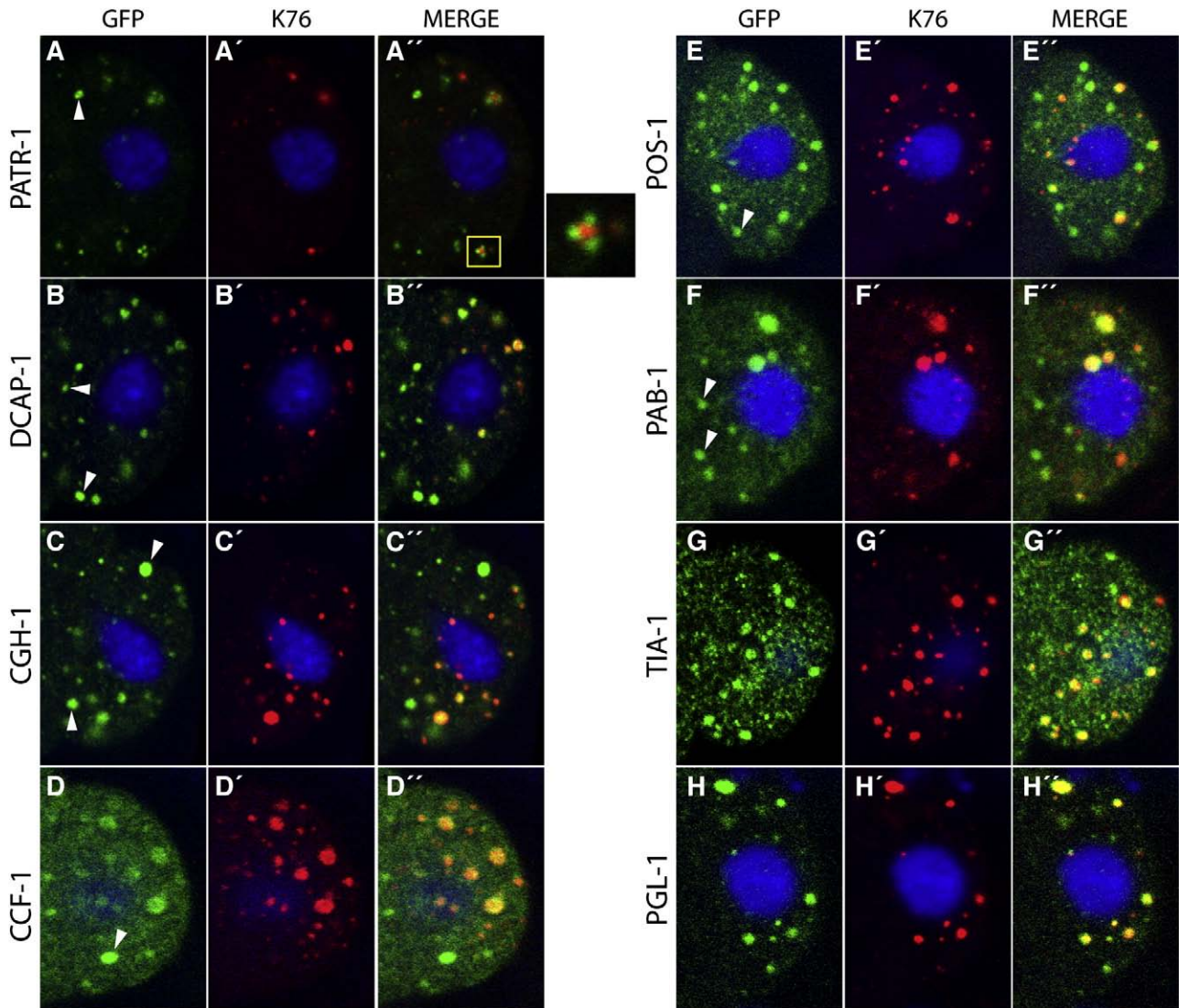
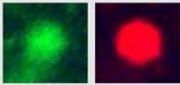
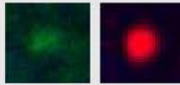

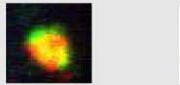
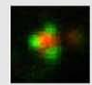


Fig. 2. Localization of P-body components in the P₂ germline blastomere. Confocal images (single focal slices) of P₂ from embryos expressing the indicated GFP fusions and double-stained with anti-GFP (green) and K76 (red) antibodies. With the exception of PGL-1 and TIA-1, all fusions localize to some granules that do not stain with K76 (white arrowheads). Insert in panel A shows close-up of a germ granule surrounded by three GFP:PATR-1 foci.

and PGL-1:GFP in live embryos (4.2 μm slices) using time-lapse microscopy (Supplementary Movies 1, 2, and 5). In the zygote prior to polarization, mCherry:PATR-1 and PGL-1:GFP granules were uniformly distributed throughout the cytoplasm. Most granules

were in closely juxtaposed pairs, containing one mCherry:PATR-1 granule and one PGL-1:GFP granule (Fig. 3E). During polarization, mCherry:PATR-1 granules remained stable and uniformly distributed. In contrast, PGL-1:GFP granules disappeared from the

Table 1
Overlap of K76 granules with P-body components

					
	Complete overlap	Weak overlap	No overlap	Partial overlap	Adjacent
GFP:PATR-1	3% (3/91)	7% (6/91)	23% (21/91)	54% (55/91)	13% (12/91)
PATR-1	0% (0/93)	0% (0/93)	42% (39/93)	23% (21/93)	35% (33/93)
GFP:DCAP-1	5% (4/85)	25% (21/85)	0% (0/85)	65% (55/85)	0% (0/85)
DCAP-2	15% (4/26)	31% (8/26)	0% (0/26)	54% (14/26)	0% (0/26)
GFP:CGH-1	49% (37/76)	5% (4/76)	0% (0/76)	46% (35/76)	0% (0/72)
GFP:PGL-1	93% (13/14)	7% (1/14)	0% (0/14)	0% (0/14)	0% (0/14)

Confocal images as in Fig. 2 were scanned for K76 granules, and each was examined for overlap with the GFP fusions indicated (or with anti-DCAP-2 and anti-PATR-1). Bold numbers reflect most common patterns for each component.

Note that GFP:PATR-1 shows the least % of complete overlap with K76 and was the only fusion to occasionally not stain K76 foci at all (no overlap category). In contrast the control fusion GFP:PGL-1 showed the higher % of complete overlap with K76, as expected since K76 recognizes PGL-1 (Kawasaki, 1998).

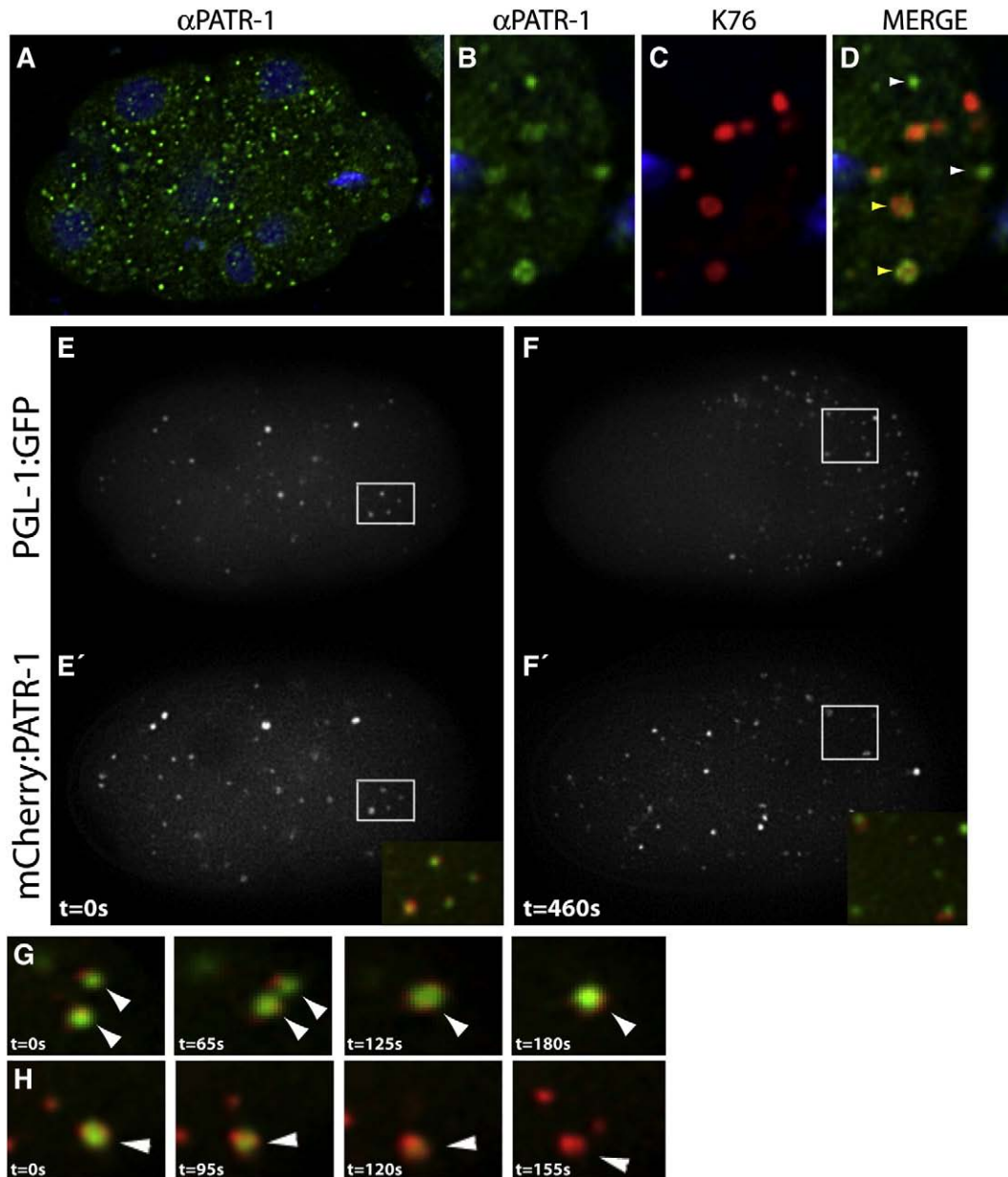


Fig. 3. PATR-1 foci associate but do not overlap with germ granules. (A) Deconvolved image (maximum Z-stack projection) of a wild-type embryo immunostained with anti-PATR-1 antibody (green) and K76 (not shown). (B–D) Close up of the P₂ blastomere from the embryo in panel A, showing PATR-1 (green) and K76 (red) immunostaining. White arrows point to PATR-1 foci that are K76 negative, and yellow arrows point to PATR-1 foci associated with a K76 granule. (E, F) Maximum projection images from a 4.2 μm stack of an embryo expressing PGL-1:GFP and mCherry:PATR-1. Images are taken from a time-lapse movie (Movie 1 in Supplementary materials). Panels E and E' shows embryo before polarization. Panels F and F' show the same embryo 460 s later during polarization. PGL-1:GFP foci are enriched in the posterior while mCherry:PATR-1 foci remains uniformly distributed. Inserts show merged mCherry:PATR-1 (red) and PGL-1:GFP (green) signals. Notice the tight but non-overlapping association between PATR-1 and PGL-1 foci. (G) Time-lapse series showing the merging of two PGL-1:GFP granules (green) with associated mCherry:PATR-1 foci (red). (H) Time-lapse series showing the disappearance of a PGL-1:GFP granule surrounded by mCherry:PATR-1 foci. The mCherry:PATR-1 foci merge into a larger granule.

anterior side of the zygote, and new PGL-1:GFP granules appeared in the posterior (Fig. 3F; Supplementary Movies 1, 2, and 5). Appearance and disappearance were gradual and accompanied by changes in size, suggesting that the granules were growing and shrinking rather than coming in and out of the 4.2 μm slice being imaged. As a result of their different dynamics, mCherry:PATR-1 granules were inherited by both the somatic (AB) and germline (P₁) daughters, whereas PGL-1:GFP granules were inherited only by the germline daughter (Supplementary Movies 1 and 2). This pattern was repeated in the P₁ blastomere (Supplementary Movie 5). In the posterior cytoplasm, PGL-1:GFP granules often collided and fused with each other, forming larger granules that retained smaller mCherry:PATR-1 granules on their surface (Fig. 3G). In 8

instances, we were able to observe the fate of these complexes when located in the anterior (somatic) side of a dividing germline blastomere. The PGL-1:GFP core shrunk and eventually disappeared. In contrast, the mCherry:PATR-1 granules remained stable and fused to form a single mCherry:PATR-1 granule to be inherited by the somatic daughter (Fig. 3H).

Time-lapse movies of embryos expressing only GFP:PATR-1 (Supplementary Movies 3 and 4) confirmed that PATR-1 foci have a different appearance in the posterior of germline blastomeres, consistent with an association with germ granules (GFP:PATR-1 localizes to small foci surrounding non-labeled cores). We conclude that PATR-1 granules interact with germ granules, but remain distinct and exhibit different dynamics.

The germ granule-associated mRNA *nos-2* does not interact stably with PATR-1 granules

nos-2 is a maternal mRNA that is translationally repressed in oocytes and early embryos. *nos-2* is degraded in somatic blastomeres starting in the 4-cell stage, and is maintained only in germline blastomeres, where a sub-pool of *nos-2* mRNA associates with germ granules (Subramaniam and Seydoux, 1999). To investigate whether *nos-2* mRNA also associates with PATR-1 bodies in germline blastomeres, we performed *in situ* hybridization experiments on embryos expressing mCherry:PATR-1.

We scored 98 mCherry:PATR-1 foci in 10 germline blastomeres. Among these, 37 were positive for K76 and were irregular in shape, presumably corresponding to multiple PATR-1 foci associated with germ granules. We found that 91% of these PATR-1/germ granule clusters were positive for *nos-2* mRNA (34/37) (Fig. 4A, yellow arrows). Unfortunately, our *in situ* hybridization protocol did not preserve the organization of the PATR-1/PGL-1 clusters, making it impossible to determine whether *nos-2* mRNA associates with a single granule type or both granule types within each cluster. However, we found that only 10% of “isolated” PATR-1 granules (mCherry-positive/K76-negative, $n=61$) were positive for *nos-2* mRNA (Fig. 4A, white arrowhead), whereas 52% of “isolated” germ granules (mCherry-negative, K76-positive $n=23$) were positive for *nos-2* RNA (Fig. 4A, inset). The control mRNA *tbb-2* did not associate with PATR-1 or K76 granules (Fig. 4B). These observations suggest that although *nos-2* mRNA may associate with PATR-1 granules in PATR-1/germ granule clusters, this association is transient and is not maintained for long in “isolated” PATR-1 granules that will be inherited by somatic blastomeres.

In somatic blastomeres, the *nos-2* FISH signal was not distinguishable from background, possibly due to the fact that *nos-2* is rapidly degraded in these cells. We observed no significant co-localization between *nos-2* and PATR-1 in somatic blastomeres (data not shown).

Maturation of PATR-1 granules in somatic blastomeres

PATR-1 granules were visible in oocytes (data not shown) and in 1-cell zygotes before polarization (Fig. 5A). DCAP-1, CGH-1, and CCF-1 granules could also be detected in zygotes, but were most prominent after polarization in the posterior cytoplasm, and were inherited primarily by P₁. Examination of GFP:DCAP-1 dynamics (Supplementary Movie 6) in zygotes confirmed that most of the DCAP-1 signal segregated to the posterior in the 1-cell stage, consistent with the fact that DCAP-1 associates with germ granules, which become asymmetrically segregated at that stage. Smaller DCAP-1 foci remained in the anterior side of the zygote, perhaps reflecting weak association with PATR-1 granules at this stage (Supplementary Movie 6). In the 2-cell stage, numerous DCAP-1, DCAP-2, and CGH-1 granules appeared in the somatic AB blastomere and by the 4-cell stage CCF-1 granules could also be detected in the two AB daughters ABA and ABp (Fig. 5F, Supplementary Movie 6, and data not shown). LSM-1 and LSM-3 were cytoplasmic in all cells until the 3/4-cell stage, when they began to concentrate in granules in ABA and ABp, and more weakly in the somatic daughter of P1, EMS (Fig. 5E and Fig. S1A). Subsequently, LSM-1 and LSM-3 foci became more abundant in EMS and its daughters as development proceeded (data not shown). Since all GFP fusions colocalized with endogenous DCAP-2 granules (Fig. 1), we hypothesize that at least some of the somatic granules contained multiple if not all of the P-body components tested. Consistent with this hypothesis, co-staining of embryos expressing GFP:LSM-1 with anti-GFP and anti-PATR-1 antibodies confirmed that at least some PATR-1 granules contain GFP:LSM-1 after the 4-cell stage (Figs. 5G–I). Furthermore removal of PATR-1 by RNAi eliminated GFP:LSM-1 granules, but not germ granules (Table 2). *patr-1(RNAi)* also caused a reduction in GFP:CGH-1 foci, but did not affect GFP:DCAP-1 foci, suggesting that PATR-1 is required for the recruitment of some but not all P-body components (data not shown).

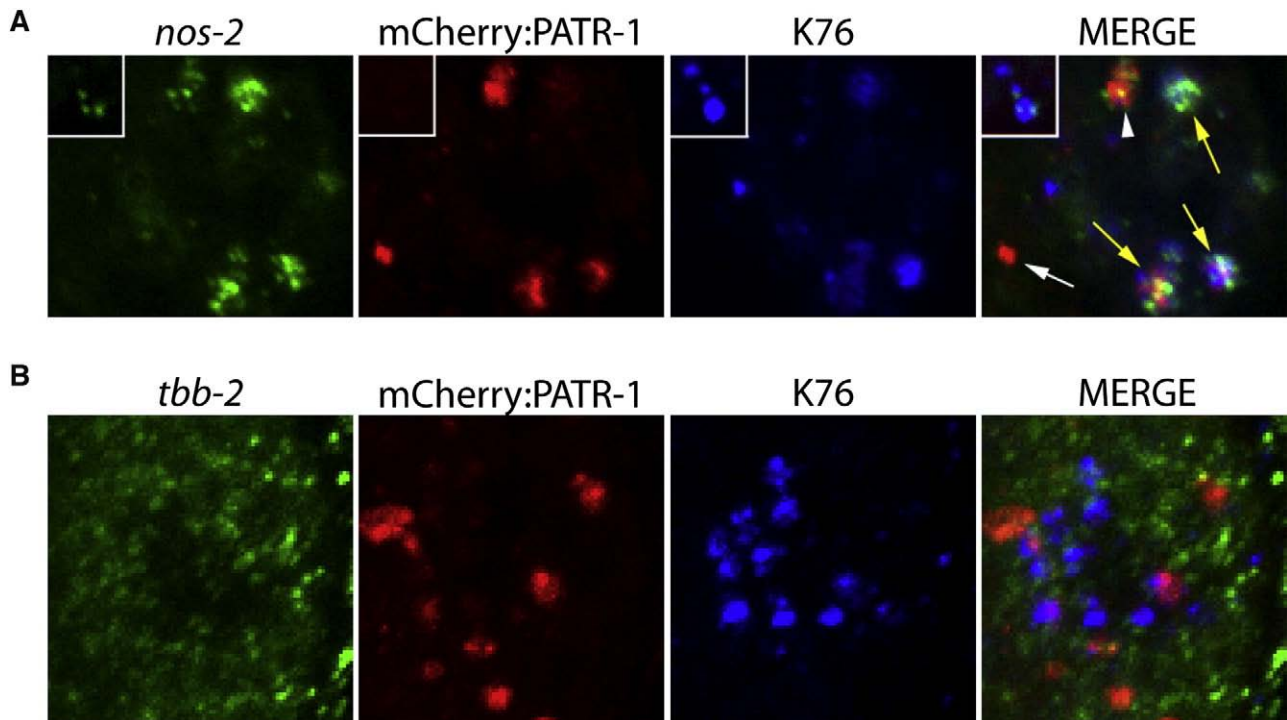


Fig. 4. *nos-2* mRNA associates with germ granules and germ granule/PATR-1 complexes, but is rarely found in isolated PATR-1 granules. (A) Deconvolved image (single focal plane) of a P₂ blastomere hybridized with *nos-2* antisense probe (green) and stained with anti-mCherry (PATR-1, red) and K76 (germ granules, blue). White arrow points to an isolated PATR-1 granule negative for *nos-2* mRNA, yellow arrows point to germ granule/PATR-1 complexes positive for *nos-2*, and white arrow head points to a rare example of a PATR-1 granule complex that is negative/low for K76 but positive for *nos-2*. Inset shows examples of isolated germ granules positive for *nos-2*. (B) As in panel A, but *in situ* probe is against *tbb-2* (tubulin) mRNA. See supplementary Fig. S3 for *nos-2* sense probe.

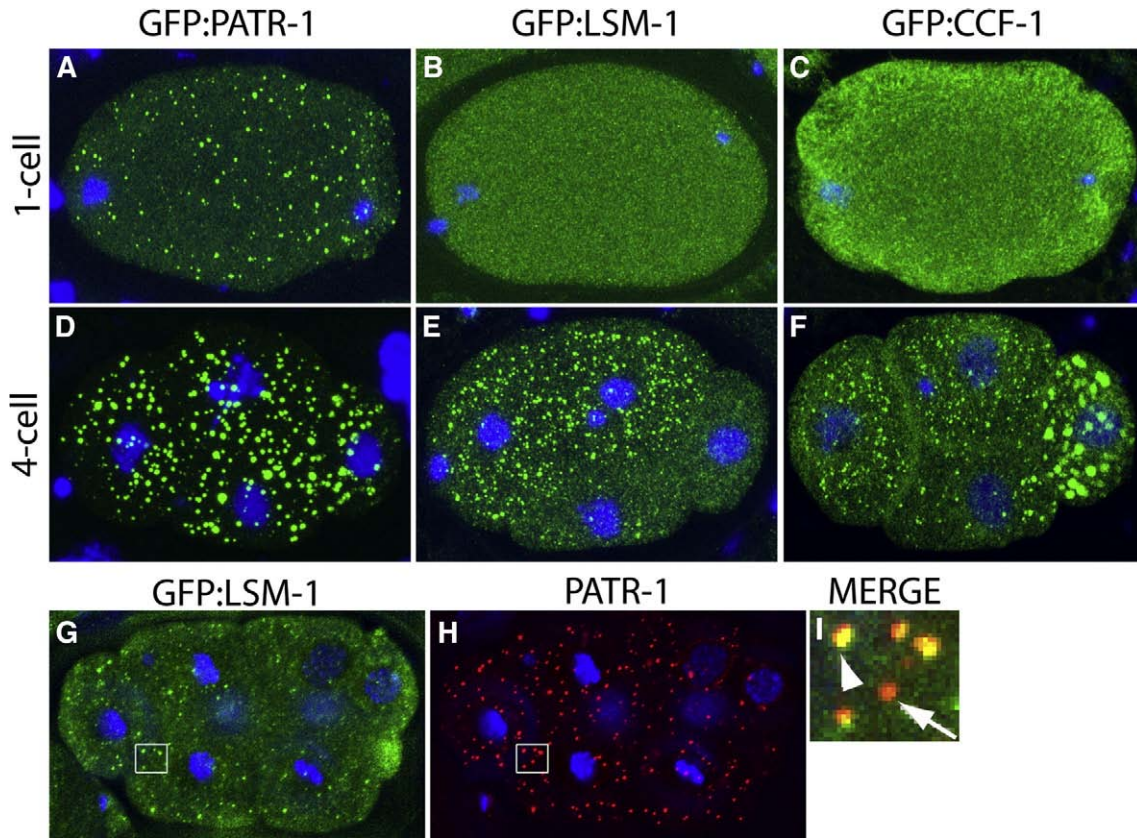


Fig. 5. PATR-1 foci are present from the 1-cell stage and recruit additional components during early cleavages. (A–F) Confocal images (maximum Z-stack projection) of fixed embryos expressing the indicated GFP fusions. Unlike PATR-1 foci, which are present in early zygotes (before pronuclear migration), LSM-1 and CCF-1 foci are not visible in early zygotes, but are clearly visible by the 4-cell stage. (G) Deconvolved image (maximum Z-stack projection) of an embryo expressing GFP:LSM-1 and immunostained for GFP and endogenous PATR-1. Merged image shows close-up of boxed region. Arrowhead points to LSM-1+/PATR-1+ granule. Arrow points to PATR-1+/LSM-1- granule.

Assembly of LSM-1 foci correlates with maternal mRNA degradation

Recruitment of cytoplasmic LSM-1 and CCF-1 to PATR-1 granules in the 4-cell stage coincides temporally and spatially with the onset of zygotic transcription and maternal mRNA degradation (Seydoux and

Fire, 1994). To determine whether recruitment of LSM-1 depends on zygotic transcription, we examined GFP:LSM-1 in embryos depleted for RNA polymerase II [*ama-1(RNAi)*]. We found that GFP:LSM-1 foci still formed in *ama-1(RNAi)* embryos (Fig. S1C), suggesting that zygotic transcription is not required. To determine whether LSM-1

Table 2
Summary of phenotypes

	WT	<i>par-1(it32)</i>	<i>mex-5/6(RNAi)</i>	<i>let-711(RNAi)</i>	<i>cgh-1(RNAi)</i>	<i>patr-1(RNAi)</i>
PATR-1 foci	All cells	All cells	All cells	All cells ^b	All cells ^a	–
LSM-1 foci	Soma only	All cells	–	–	–	–
<i>nos-2</i> mRNA degradation	Soma only	All cells	–	–	Soma only	Soma only
H2B:<i>nos-2</i> in embryos	ON in P4	OFF	ON in all cells	ON in P4 ^c	ON in P4 ^c	ON in P4
Germ granules	P blastomeres	–	–	P blastomeres ^c	P blastomeres ^c	P blastomeres

Wild-type phenotypes are highlighted in grey. Notice that formation of LSM-1 foci correlates with *nos-2* degradation in *par-1(it32)*, *mex-5/6(RNAi)* and *let-711(RNAi)* but not in *cgh-1(RNAi)* or *patr-1(RNAi)*. Expression of H2B:*nos-2* 3'UTR transgene in P₄ correlates with maintenance of germ granules.

^aOccasionally abnormal shape.

^bReduced in size.

^cOccasionally present in additional cell(s). *let-711* and *cgh-1* embryos do not divide normally.

granule formation correlates with maternal mRNA degradation, we examined GFP:LSM-1 in mutants that disrupt maternal mRNA degradation (Fig. 6). In these experiments, we monitored maternal mRNA degradation using *in situ* hybridization against *nos-2*, which is degraded in somatic blastomeres starting in the 4-cell stage (Subramaniam and Seydoux, 1999), *par-1* (Guo and Kemphues, 1995) and the redundant *mex-5* and *mex-6* (Schubert et al., 2000) are polarity regulators that have opposite effects on *nos-2* mRNA degradation. In *par-1* mutant embryos, *nos-2* was degraded throughout the embryo and LSM-1 granules formed in all blastomeres (Figs. 6B, F). In embryos co-depleted for MEX-5 and MEX-6, *nos-2* was not degraded and LSM-1 foci did not form in any blastomere (Figs. 6C, G). PATR-1 granules, however, could still be detected (Fig. 6K). Next we depleted *let-711*/Not1, a component with CCF-1 of the CCR4-NOT deadenylase complex implicated in mRNA degradation (reviewed in Collart and Timmers, 2004; DeBella et al., 2006) and required for embryonic development in *C. elegans* (DeBella et al., 2006). Depletion of *let-711*/Not1 efficiently blocked *nos-2* degradation (Fig. 6D). This treatment also blocked recruitment of LSM-1 (Fig. 6H) and reduced the intensity/number of PATR-1 granules in somatic blastomeres (Fig. 6L). We conclude that LET-711, and likely the CCR4-NOT deadenylase complex, is required for *nos-2* degradation, and formation/stabilization of PATR-1/LSM-1 granules. We note however that formation of visible GFP:LSM-1 granules is not essential for mRNA degradation, since these were not visible in *cgh-1(RNAi)* and *patr-1(RNAi)*, which were still competent for *nos-2* mRNA degradation (Table 2).

Translational repression of *nos-2* in oocytes requires CGH-1 and LET-711

In addition to regulation by degradation, *nos-2* mRNA is also regulated at the level of translation. *nos-2* mRNA is translationally repressed in oocytes and early embryos. *nos-2* translation is activated

in the 28-cell stage in the germline blastomere P₄, the only blastomere that retains *nos-2* mRNA at that stage (Subramaniam and Seydoux, 1999). Regulation of *nos-2* translation depends on sequences in its 3' UTR, and a *GFP:H2B:nos-2 3'UTR* transgene faithfully recapitulates this regulation. GFP:H2B is not present in oocytes and is first detected in embryos in P₄ and its descendants Z2 and Z3 (Fig. 7) (D'Agostino et al., 2006). We found that depletion of LET-711 and CGH-1 activated translation of *GFP:H2B:nos-2 3'UTR* prematurely in oocytes (Figs. 7B, G). These treatments, however, did not prevent silencing of the transgene in early embryos (Figs. 7C, D) or activation in P₄ (and its two daughters) in older embryos (Figs. 7E and F). This was true even in the case of *let-711(RNAi)* which stabilizes *nos-2* mRNA in all blastomeres (Fig. 6D), but activated *GFP:H2B:nos-2 3'UTR* only 1–2 blastomeres in 28-cell and older embryos (Fig. 7F), as is observed in wild-type. We conclude that 1) translational repression of *nos-2* mRNA in oocytes requires CGH-1 and LET-711, and 2) translational repression in early embryos and activation in P₄ likely occur independently of these factors.

Discussion

P-bodies mature differently in somatic versus germline blastomeres

Based on our analysis of the distribution of six P-body components, we propose the following model to describe P-body dynamics in early *C. elegans* embryos (Fig. 8). P-bodies are inherited maternally as core granules containing PATR-1. These granules are segregated equally during early cleavages, but recruit different components in somatic versus germline blastomeres. In somatic blastomeres, P bodies recruit LSM-1 and LSM-3 coincident with the onset of maternal degradation. In germline blastomeres, which do not degrade maternal mRNAs, P bodies recruit PAB-1 and associate with germ granules. Our findings

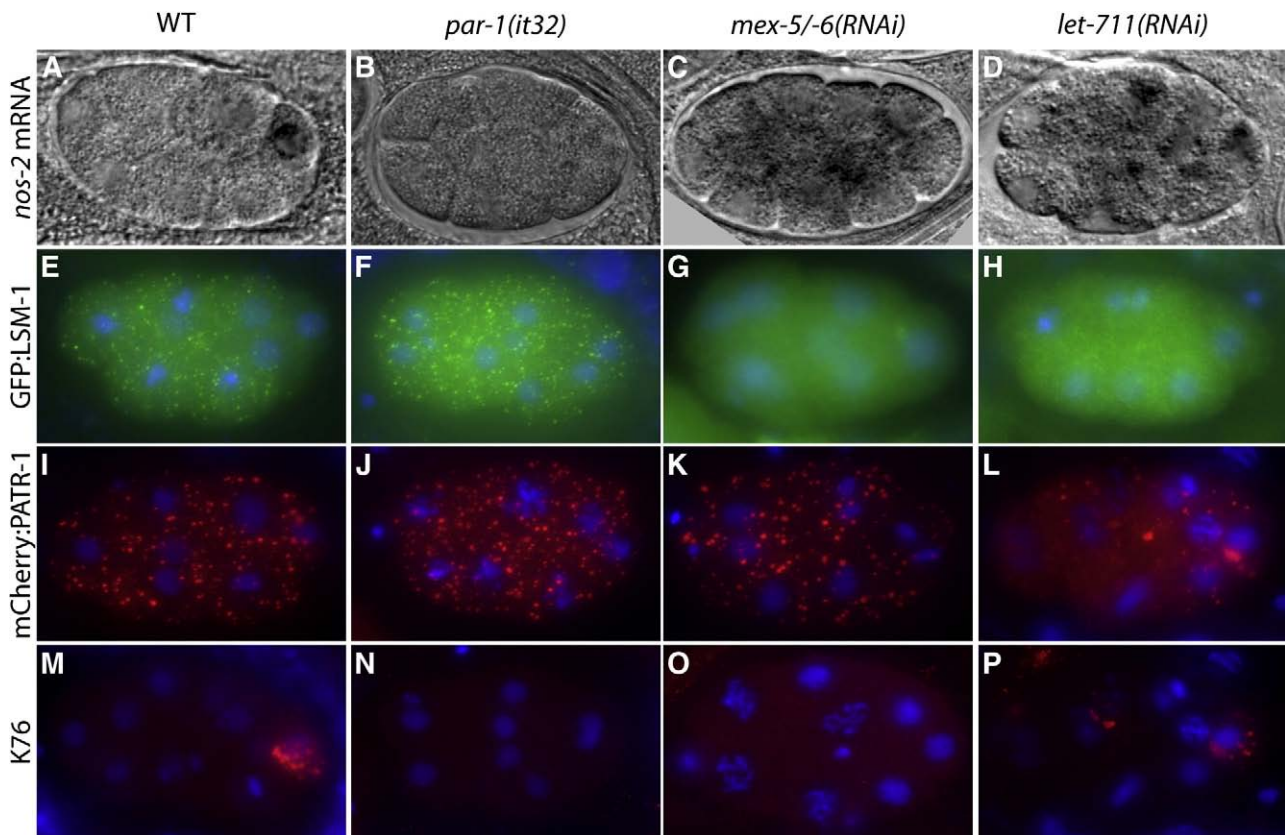


Fig. 6. Formation of LSM-1 foci correlates with maternal mRNA degradation. (A–D) *In situ* hybridization of *nos-2* mRNA (black) in wild-type (WT) and mutant embryos. (E–P) Wide-field fluorescence images (maximum Z-stack projections) of fixed embryos of indicated genotype and expressing indicated fusions (or no fusion M–P) stained with anti-GFP (E–H), anti-DsRed (I–L), or K76 (M–P). PATR-1 granules are present in all genotypes. K76 granules are present only in WT and *let-711(RNAi)*.

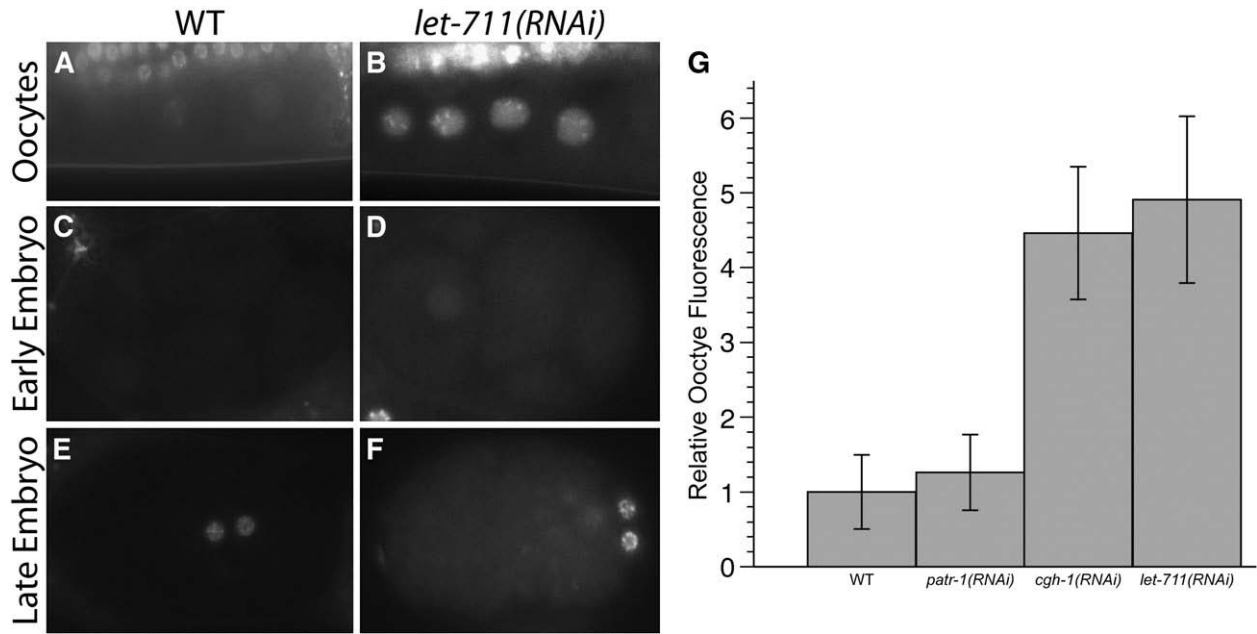


Fig. 7. Depletion of *let-711* and *cgh-1* activates *nos-2* reporter prematurely in oocytes but does not affect its regulation in embryos. (A-F) Live images of GFP:H2B::*nos-2* 3'UTR transgene in wild-type and *let-711(RNAi)*. (A, B) Oocytes; (C, D) 4-cell embryo; (E, F) ~50-cell embryo. The transgene is activated in 2 cells in late embryos, these two cells likely correspond to the two P4 daughters, the primordial germ cells Z2 and Z3. (G) Graphs showing relative increase in GFP:H2B fluorescence in oocytes of indicated genotype relative to wild-type (set to 1).

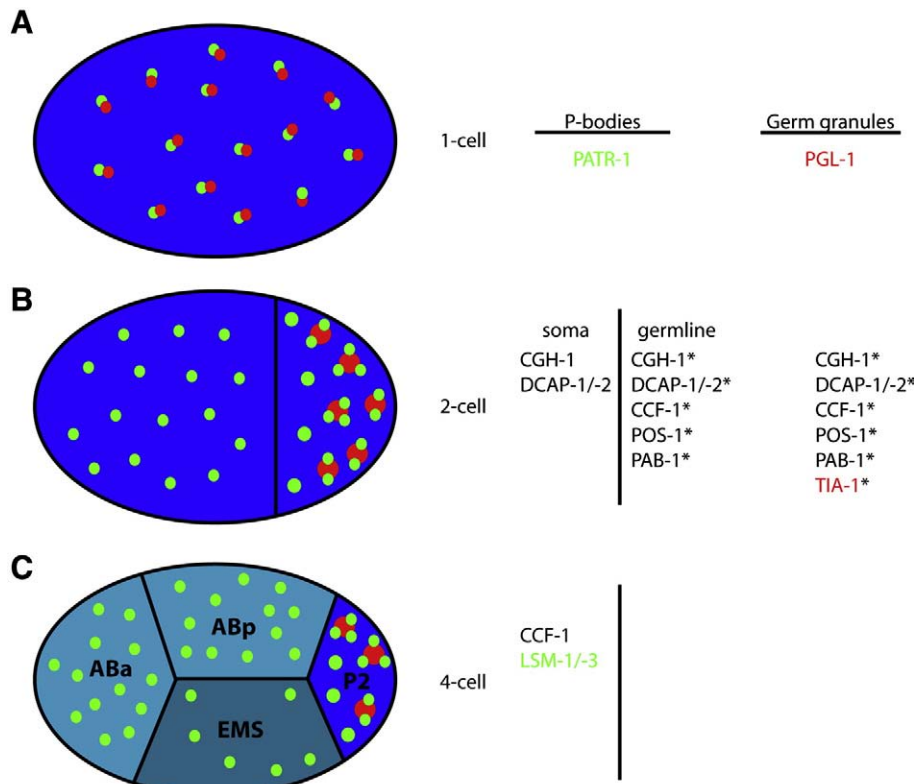


Fig. 8. Model for P-body and germ granule dynamics during early cleavages. Schematic of 1, 2 and 4-cell embryos with P-bodies in green and germ granules in red. Maternal mRNAs are indicated by blue color. For each stage, proteins recruited to each granule type are indicated on the right (green: proteins detected only in P-bodies, red: proteins detected only in germ granules, black: proteins detected in both). (A) One cell zygote before polarization. Maternally-inherited "core" P-bodies, marked by PATR-1, are uniformly distributed, and paired with germ granules, marked by PGL-1. (B) At the two-cell stage, P-bodies are inherited by both blastomeres. Germ granules are maintained only in the germline blastomere, where they fuse to form larger granules. New proteins appear on P-bodies and germ granules at this stage, although since several exhibit high cytoplasm/granule ratios (asterisks), we cannot exclude the possibility that these were already present in the smaller, harder to detect P-bodies and/or germ granules of the zygote. (C) During the transition from the 2 to 4-cell stage, P-bodies become competent for degradation and acquire CCF-1 and LSM proteins, first in the AB blastomeres (born in the 3-cell stage) and then in EMS (born in the 4-cell stage). The onset of mRNA degradation (lighter blue shades) correlates with P-body maturation. P-bodies do not recruit LSM-1/3 in germline blastomeres, where maternal mRNAs remain stable.

demonstrate that P-bodies are dynamic structures that change composition during development.

In somatic blastomeres, P-bodies recruit activators of mRNA decapping and deadenylation, coincident with the onset of maternal mRNA degradation

P-bodies in somatic blastomeres appear to recruit all the P-body components we tested, although we do not know whether every individual P-body contains all components. The last proteins to be recruited (4-cell stage) were the deadenylase subunit CCF-1 and the decapping activators LSM-1 and LSM-3, implicated in mRNA degradation in yeast and *Drosophila* (Semotok et al., 2005; Tharun et al., 2000). Several lines of evidence suggest that formation of “complete P-bodies” containing LSM proteins correlates with the onset of maternal mRNA degradation. First complete P-bodies appear at the right time and place, since maternal mRNA degradation begins in the 4-cell stage and specifically in somatic blastomeres. Second the pattern of LSM-1 foci formation was not affected by depletion of RNA polymerase II, but was changed by treatments that block maternal mRNA degradation (no LSM foci) or cause it to occur in all blastomeres (LSM foci in all cells). Finally, formation of LSM-1 foci and maternal mRNA degradation were both dependent on LET-711/Not1, a core subunit with CCF-1 of the CCR4-NOT deadenylase complex. Together these observations support the view that PATR-1 foci mature in somatic blastomeres into “complete P-bodies” that contain many components required for maternal mRNA degradation. The recruitment of LSM proteins to P-bodies may mark those that are degradation competent, since not all somatic PATR-1 foci contained GFP:LSM-1 (Figs. 5G–I). We note, however, that formation of visible “complete P-bodies” is unlikely to be essential for maternal mRNA degradation, since RNAi depletion of PATR-1 and CGH-1 (Table 2) and DCAP-2 and LSM-1 (data not shown) eliminates visible LSM-1 foci without affecting maternal mRNA degradation. One possibility is that RNAi depletion is inefficient, leading to the formation of sub-microscopic granules sufficient for mRNA degradation (Decker et al., 2007; Eulalio et al., 2007). Consistent with our results, however, Lall et al., 2006 have reported that strong depletion of DCAP-2 by RNAi does not cause visible phenotypes in embryos. A likely alternative is that maternal mRNA degradation depends redundantly on P-bodies and other RNA degradation pathways. Consistent with this possibility, we have found that exosome components are enriched in somatic blastomeres (Fig. S1B). In yeast, deletion of Lsm1, Dhh1 (CGH-1), and Pat1 (PATR-1) inhibit, but do not eliminate, mRNA decay (Coller et al., 2001; Tharun et al., 2000), suggesting that redundancy may be common in eukaryotes.

In germline blastomeres, P-bodies recruit poly-A binding protein and interact with germ granules

In germline blastomeres, PATR-1 foci do not recruit LSM-1 and LSM-3, but still contain CGH-1, DCAP-1, DCAP-2, CCF-1, and additionally recruit the poly(A)-binding protein PAB-1, also found in germ granules. Poly(A)-binding protein is a stress granule component in mammalian cells (Kedersha et al., 1999). In yeast, poly(A)-binding protein accumulates in P-bodies only under stress conditions, when poly-adenylated mRNAs also enter P-bodies (Bregues and Parker, 2007). Since germ granules are known to contain poly-adenylated mRNAs (Seydoux and Fire, 1994), one possibility is that P-bodies capture these mRNAs (and PAB-1) while docked on germ granules. This process may be particularly efficient in the anterior cytoplasm of dividing germline blastomeres, where germ granules shrink and disperse, while P-bodies remain stable. Although it seems likely that germ granules and P-bodies exchange certain mRNAs and even certain proteins (e.g. CGH-1 and PAB-1), our findings strongly suggest that the two granules remain distinct and maintain different dynamics and

components. The germ granule RNA *nos-2* may associate transiently with P-bodies when docked on germ granules, but does not appear to be maintained stably in free P-bodies. The observation that depletion of CGH-1 and LET-711 activates *nos-2* translation in oocytes without affecting *nos-2* regulation in germline blastomeres is also consistent with the existence of separable regulatory mechanisms acting on maternal mRNAs. CGH-1 is primarily cytoplasmic in oocytes (Navarro et al., 2001), suggesting that it exerts its effect on the cytoplasmic pool of *nos-2* mRNA, and that different factors (or combination of factors) control the expression of the germ-granule protected pool of *nos-2* in embryos. Consistent with this view, separate sequences in the *nos-2* 3' UTR are required for translational regulation in oocytes versus embryos (D'Agostino et al., 2006).

Parallels between germ granules and stress granules

P-bodies have been reported to interact with stress granules in mammalian cells (Kedersha et al., 2005). Several lines of evidence suggest parallels between germ granules and stress granules. 1) Both share components with P-bodies, but additionally also contain unique factors. In mammalian cells, TIA-1 is a marker of stress granules, and we show here that a GFP:TIA-1 fusion is enriched on germ granules in *C. elegans*. 2) Germ granules and stress granules are dynamic. Stress granules assemble within minutes of stress exposure and dissipate after recovery. Similarly, germ granules grow and disperse during each asymmetric division in the germline blastomeres. Germ granules have also been reported to appear in somatic cells under conditions of transcriptional deregulation (Wang et al., 2005). 3) Stress granules store mRNAs that are translationally repressed. The translationally-repressed *nos-2* mRNA associates with germ granules, and does not appear to associate stably with P-bodies. 4) P-bodies dock on stress granules in mammalian cells, and P-bodies dock on germ granules in germline blastomeres. We note that, although germ granules and stress granules share certain characteristics, they also differ in other respects. For example, stress granules contain small ribosomal proteins, which we have not observed in germ granules (C. G., unpublished), and germ granules associate with nuclei, a characteristic not reported for stress granules (reviewed in Anderson and Kedersha, 2006).

Interactions between stress granules and P-bodies have been suggested to stimulate transfer of mRNAs from stress granules to P-bodies for degradation (Kedersha et al., 2005). A similar mechanism may be operating in germline blastomeres, with germ granules and P-bodies competing for the same maternal mRNAs. Since P-bodies lack LSM proteins until in somatic blastomeres, germ granule mRNAs captured by P-bodies are unlikely to be degraded immediately, but may be tagged for degradation after cell division in the somatic daughter. In yeast, mRNAs in P-bodies can also reenter the polysome pool under certain conditions (Bregues et al., 2005). Capture by P-bodies, therefore, could also help promote the transfer of germ granule mRNAs to polysomes for translation. *nos-2* regulation depends on the CCCH finger proteins OMA-1/2, MEX-5/MEX-6 and POS-1 (D'Agostino et al., 2006; Jadhav et al., 2008). These proteins belong to the same class of RNA binding proteins as TTP, which stimulates P-body/stress granules interactions in mammalian cells (Kedersha et al., 2005). An intriguing possibility is that CCCH finger proteins regulate the fate of germ granules mRNAs by modulating their affinity for germ granules and/or P-bodies. An important challenge for the future will be to determine the mechanisms that regulate mRNA trafficking in and out of germ granules and P-bodies and whether similar interactions exist in the germline of other organisms.

Acknowledgments

We thank K. Kemphues for the *par-1(it32)* line, J. Priess and U. Wolke for the PGL-1:GFP line, R. Davis for the anti-DCAP-2 antibody,

and M. Stitzel and E. Voronina for their comments on the manuscript. Some nematode strains used in this work were provided by the *Caenorhabditis* Genetics Center, which is funded by the NIH National Center for Research Resources (NCRR). The K76 antibody developed by Strome and Wood was obtained from the Developmental Studies Hybridoma Bank (under the auspices of the NICHD and maintained by The University of Iowa, Department of Biological Sciences, Iowa City, IA 52242). This work was supported by NIH grants GM080042 to C.G., GM066050 to E.M., and HD037047 to G.S. G.S. is a Howard Hughes Medical Institute investigator.

Appendix A. Supplementary data

Supplementary data associated with this article can be found, in the online version, at doi:10.1016/j.ydbio.2008.07.008.

References

- Anderson, P., Kedersha, N., 2006. RNA granules. *J. Cell. Biol.* 172, 803–808.
- Audhya, A., et al., 2005. A complex containing the Sm protein CAR-1 and the RNA helicase CGH-1 is required for embryonic cytokinesis in *Caenorhabditis elegans*. *J. Cell. Biol.* 171, 267–279.
- Bashkurov, V.I., et al., 1997. A mouse cytoplasmic exoribonuclease (mXRNP1) with preference for G4 tetraplex substrates. *J. Cell. Biol.* 136, 761–773.
- Boag, P.R., et al., 2005. A conserved RNA-protein complex component involved in physiological germline apoptosis regulation in *C. elegans*. *Development* 132, 4975–4986.
- Bregues, M., Parker, R., 2007. Accumulation of polyadenylated mRNA, Pab1p, eIF4E, and eIF4G with P-bodies in *Saccharomyces cerevisiae*. *Mol. Biol. Cell.* 18, 2592–2602.
- Bregues, M., et al., 2005. Movement of eukaryotic mRNAs between polysomes and cytoplasmic processing bodies. *Science* 310, 486–489.
- Brenner, S., 1974. The genetics of *Caenorhabditis elegans*. *Genetics* 77, 71–94.
- Cheeseman, I.M., et al., 2004. A conserved protein network controls assembly of the outer kinetochore and its ability to sustain tension. *Genes Dev.* 18, 2255–2268.
- Collart, M.A., Timmers, H.T., 2004. The eukaryotic Ccr4-not complex: a regulatory platform integrating mRNA metabolism with cellular signaling pathways? *Prog. Nucleic. Acid. Res. Mol. Biol.* 77, 289–322.
- Coller, J.M., et al., 2001. The DEAD box helicase, Dhh1p, functions in mRNA decapping and interacts with both the decapping and deadenylase complexes. *RNA* 7, 1717–1727.
- D'Agostino, I., et al., 2006. Translational repression restricts expression of the *C. elegans* Nanos homolog NOS-2 to the embryonic germline. *Dev. Biol.* 292, 244–252.
- DeBella, L.R., et al., 2006. LET-711, the *Caenorhabditis elegans* NOT1 ortholog, is required for spindle positioning and regulation of microtubule length in embryos. *Mol. Biol. Cell* 17, 4911–4924.
- Decker, C.J., et al., 2007. Edc3p and a glutamine/asparagine-rich domain of Lsm4p function in processing body assembly in *Saccharomyces cerevisiae*. *J. Cell Biol.* 179, 437–449.
- Eddy, E.M., 1975. Germ plasm and the differentiation of the germ cell line. *Int. Rev. Cytol.* 43, 229–280.
- Eulalio, A., et al., 2007. P-body formation is a consequence, not the cause, of RNA-mediated gene silencing. *Mol. Cell Biol.* 27, 3970–3981.
- Guo, S., Kempf, K.J., 1995. par-1, a gene required for establishing polarity in *C. elegans* embryos, encodes a putative Ser/Thr kinase that is asymmetrically distributed. *Cell* 81, 611–620.
- Jadhav, S., et al., 2008. Multiple maternal proteins coordinate to restrict the translation of *C. elegans* nanos-2 to primordial germ cells. *Development* 135, 1803–1812.
- Kamath, R.S., Ahringer, J., 2003. Genome-wide RNAi screening in *Caenorhabditis elegans*. *Methods* 30, 313–321.
- Kawasaki, I., et al., 1998. PGL-1, a predicted RNA-binding component of germ granules, is essential for fertility in *C. elegans*. *Cell* 94, 635–645.
- Kedersha, N., et al., 2005. Stress granules and processing bodies are dynamically linked sites of mRNP remodeling. *J. Cell Biol.* 169, 871–884.
- Kedersha, N.L., et al., 1999. RNA-binding proteins TIA-1 and TIAR link the phosphorylation of eIF-2(α) to the assembly of mammalian stress granules. *J. Cell Biol.* 147, 1431–1442.
- Kotaja, N., et al., 2006. The chromatoid body of male germ cells: similarity with processing bodies and presence of Dicer and microRNA pathway components. *Proc. Natl. Acad. Sci. U. S. A.* 103, 2647–2652.
- Lall, S., et al., 2005. *Caenorhabditis elegans* decapping proteins: localization and functional analysis of Dcp1, Dcp2, and DcpS during embryogenesis. *Mol. Biol. Cell* 16, 5880–5890.
- Landy, A., 1989. Dynamic, structural, and regulatory aspects of lambda site-specific recombination. *Annu. Rev. Biochem.* 58, 913–949.
- Lin, M.D., et al., 2006. *Drosophila* decapping protein 1, dDcp1, is a component of the oskar mRNP complex and directs its posterior localization in the oocyte. *Dev. Cell* 10, 601–613.
- Mello, C.C., et al., 1996. The PIE-1 protein and germline specification in *C. elegans* embryos. *Nature* 382, 710–712.
- Nakamura, A., et al., 2001. Me31B silences translation of oocyte-localizing RNAs through the formation of cytoplasmic RNP complex during *Drosophila* oogenesis. *Development* 128, 3233–3242.
- Navarro, R.E., et al., 2001. cgh-1, a conserved predicted RNA helicase required for gametogenesis and protection from physiological germline apoptosis in *C. elegans*. *Development* 128, 3221–3232.
- Parker, R., Sheth, U., 2007. P bodies and the control of mRNA translation and degradation. *Mol. Cell* 25, 635–646.
- Praitis, V., et al., 2001. Creation of low-copy integrated transgenic lines in *Caenorhabditis elegans*. *Genetics* 157, 1217–1226.
- Schisa, J.A., et al., 2001. Analysis of RNA associated with P granules in germ cells of *C. elegans* adults. *Development* 128, 1287–1298.
- Schubert, C.M., et al., 2000. MEX-5 and MEX-6 function to establish soma/germline asymmetry in early *C. elegans* embryos. *Mol. Cell* 5, 671–682.
- Semotok, J.L., et al., 2005. Smaug recruits the CCR4/POP2/NOT deadenylase complex to trigger maternal transcript localization in the early *Drosophila* embryo. *Curr. Biol.* 15, 284–294.
- Seydoux, G., Braun, R.E., 2006. Pathway to totipotency: lessons from germ cells. *Cell* 127, 891–904.
- Seydoux, G., Fire, A., 1994. Soma-germline asymmetry in the distributions of embryonic RNAs in *Caenorhabditis elegans*. *Development* 120, 2823–2834.
- Sheth, U., Parker, R., 2003. Decapping and decay of messenger RNA occur in cytoplasmic processing bodies. *Science* 300, 805–808.
- Squirrell, J.M., et al., 2006. CAR-1, a protein that localizes with the mRNA decapping component DCAP-1, is required for cytokinesis and ER organization in *Caenorhabditis elegans* embryos. *Mol. Biol. Cell* 17, 336–344.
- Strome, S., 2005. Specification of the germ line. *WormBook* 1–10.
- Strome, S., Wood, W.B., 1983. Generation of asymmetry and segregation of germ-line granules in early *C. elegans* embryos. *Cell* 35, 15.
- Subramaniam, K., Seydoux, G., 1999. nos-1 and nos-2, two genes related to *Drosophila* nanos, regulate primordial germ cell development and survival in *Caenorhabditis elegans*. *Development* 126, 4861–4871.
- Tabara, H., et al., 1999. pos-1 encodes a cytoplasmic zinc-finger protein essential for germline specification in *C. elegans*. *Development* 126, 1–11.
- Tharun, S., et al., 2000. Yeast Sm-like proteins function in mRNA decapping and decay. *Nature* 404, 515–518.
- Wang, D., et al., 2005. Somatic misexpression of germline P granules and enhanced RNA interference in retinoblastoma pathway mutants. *Nature* 436, 593–597.
- Wolke, U., et al., 2007. Actin-dependent cytoplasmic streaming in *C. elegans* oogenesis. *Development* 134, 2227–2236.
- Yamasaki, S., et al., 2007. T-cell intracellular antigen-1 (TIA-1)-induced translational silencing promotes the decay of selected mRNAs. *J. Biol. Chem.* 282, 30070–30077.